RESEARCH ARTICLE OPEN ACCESS

Computational Fluid Dynamics (CFD) Analysis of Natural Convection of Convergent-Divergent Fins in Marine Environments

K. Alawadhi*, Abdulwahab J. Alsultan**, S. Joshi***, M. Sebzali****, Esam. AM.Husain

*(Department of Automotive and Marine Technology, The Public Authority for Applied Education and Training, Showaikh, Kuwait)

**(The Higher Institute of Energy Water Resource Department, The Public Authority for Applied Education and Training, Kuwait City, Kuwait)

***(Department of Mechanical and Industrial Engineering, Concordia University, 1515 St. Catherine Street W, Montreal, QC H3G 2W1,Canada)

****(Kuwait Institute for Scientific Research (KISR), Showaikh, Kuwait)

*****Department of Automotive and Marine Technology, The Public Authority for Applied Education and Training, P.O. Box 42325, Shuwaikh, Kuwait City 70654, Kuwait

ABSTRACT

Computational Fluid Dynamics (CFD) analysis was carried out for the convergent-divergent fins arranged inline and staggered on the base plate as per the experimental setup provided in the technical paper [1]. This paper reports on the validation of results of modeling and simulation in CFD. The simulation was carried out using the ANSYS 12.0 as the CFD modeling software. The main objective of the CFD analysis was to calculate the temperature distribution on the surface of the base plate and surface of the convergent-divergent fins for the given inline and staggered arrangement of fins due to the effect of natural convection heat transfer for different heat power inputs, and also to compare the CFD results with the experimental results.

Keywords **-** CFD simulation, Convergent-divergent fins, Heat sink, Natural convection, Surface augmentation.

I. Introduction

Fins are widely used in the trailing edges of marine ships, gas-turbine blades, electronic cooling and the aerospace industry. They are commonly employed as a means to increase the heat transfer surface area in order to augment the rate of heat transfer from the surface to the surrounding air. In heat exchange applications, many different types of fins are used in accordance with the shape of the primary surface.

Improvements in heat transfer can be accomplished by several means, viz. (i) by increasing the heat transfer surfaces, (ii) increasing the difference in temperatures between two media of interest, or (iii) by increasing the coefficients of heat transfer. The last two of the three, i.e., increasing the temperature difference or increasing the heat transfer coefficient, are relatively different to accomplish; therefore, increasing the heat transfer surface area becomes an applicable solution in order to improve the heat transfer.

The relative fin height (H/d) affects the heat transfer of pin-fins, and other affecting factors include the velocity of fluid flow, the thermal properties of the fluid, the cross-sectional shape of the pin-fins like perforation, the relative inter-fin pitch, the arrangement of the pin-fins, such as inline, staggered arrangement, and others [2].

Computational Fluid Dynamics (CFD) can simultaneously predict airflow, heat transfer and contaminant transport in and around fins. A CFD model is built on fundamental physical equations of fluid flow and energy transfer. The technique is capable of providing time dependent as well as steady state solutions to the coupled differential equations that govern fluid flows. Its key benefits include an ability to represent the effects of very complex geometries, coupled with a means to solve complex flow problems based on a more fundamental modeling of the physics involved. It has since been developed and applied to an increasingly diverse range of problems, including automotive, aerospace, nuclear engineering, turbo machinery, biomedical field, buildings, environment, and fire safety engineering.

Du and Yang [3] conducted an investigation on heat transfer and pressure drop characteristics of fin-and-tubes with three kinds of different but closely related air-side fin configurations were made by numerical simulation. Asim et al. [4] used CFD-based techniques to analyze the effects of the

number of blades within the stator and rotor of an in-house built Vertical Axis Marine Current Turbine on the performance output of the turbine. Sigurdsson et al. [5] presented a novel CFD model for the study of the scavenging process and convective heat transfer in a large two-stroke, low-speed uniflow-scavenged marine diesel engine. Their results showed an effective scavenging and a low convective heat loss in accordance with experimental data for large marine diesel engines.

As is evident from the above work, a number of assumptions and approximations have been made, both in formulating and constructing a CFD tool as well as in its application to a particular flow problem. Compromises are also often required in order to achieve reasonable run-times. All these factors ultimately influence the reliance which can be placed on the results of CFD simulations. With the help of the CFD technique, engineers can calculate the airflow distributions in and around buildings, and architects can use the resultant information to modify their designs. The CFD technique allows engineers to quickly and inexpensively analyze airflows in and around buildings and the information can help architects to design buildings that can be more effectively ventilated during the summer and the monsoon to achieve better thermal comfort. More information can be found in general books on CFD, e.g. [6 - 8].

When applying a CFD package to undertake a flow and thermal analysis, there are a number of steps involved for completing the CFD process, viz:

- Defining the geometry and domain
- Selecting physical sub-models
- Specifying boundary conditions at the frontiers of the domains including walls, window openings and material properties
- Discretizing the mathematical equations, which includes creating a mesh (which sub-divides the space into small volumes), setting time steps (which divides the time into discrete steps), and selecting numerical sub-models
- Monitoring the iterative solution process
- Analyzing the solution obtained
- Uncertainties that may arise at each of these steps
- Visualizing the obtained solution

II. Governing Equations

Governing Equations (Navier-Stokes equations) are important in any fluid flow problems. The objective, in this scenario, was to build a mathematical representation of a 3-d model and numerically solve the 3-d Navier-Stokes equations over a discretized flow field, based on the finite volume method. Incompressible N-S equations were used for simulating the air flow movement, temperature variations, and relative humidity.

The general conservation of mass equation states that the rate of mass storage within a given control volume, due to density changes, is balanced by the net rate of inflow of mass by convection. In the case of a steady flow situation, the conservation of mass equation states that what flows in must come out [9]. The equation is:

$$\frac{\partial \rho}{\partial t} + \nabla . \rho u = 0 \qquad (1)$$

where the first term describes the density changes with time and the second term defines the mass convection, and **u** is the vector describing the velocity in the u, v and w directions. The equation for the conservation of momentum is derived by applying Newton's second law of motion, which states that the rate of momentum of a fluid element is equal to the sum of the forces acting on it [9]. The equation is:

$$\rho\left(\frac{\partial u}{\partial t} + (u.\nabla)u\right) = -\nabla p + \nabla . \tau + \rho g + f \qquad (2)$$

In this case, the left hand side represents the increase in momentum and inertia forces, while the right hand side comprises the forces acting. These forces include the pressure *p*, the gravity *g*, an external force vector *f* (which represents the drag associated with sprinkler droplets that penetrate the control volume) and a measure of the viscous stress tensor τ acting on the fluid within the control volume. Among these forces, gravity is most important because it represents the influence of buoyancy on the flow.

The equation for conservation of energy is the first law of thermodynamics which states that increase in energy of the control volume is equal to the heat added minus the work done by expansion. The conservation of energy is in the form of:

$$\rho\left(\frac{\partial u}{\partial t} + (u.\nabla)u\right) = -\nabla p + \nabla . \tau + \rho g + f \qquad (3)$$

where k_{eff} is the effective thermal conductivity, $\overrightarrow{J_J}$ is the diffusion flux of species 'j'. The first three terms on the right hand side of the above equation represents energy transfer due to conduction, species diffusion and viscous dissipation respectively, *S* includes the heat of chemical reaction and any other defined volumetric heat sources.

In the above equation:

$$E = h - \frac{p}{\rho} + \frac{v^2}{2} \qquad (4)$$

where sensible enthalpy *h* is defined for ideal gases as:

$$h = \sum_j Y_j h_j \qquad (5)$$

and for incompressible flow as:

$$h = \sum_j Y_j h_j + \frac{p}{\rho} \qquad (6)$$

Y_j is the mass function of species *j* and:

$$h_j = \int_{T_{ref}}^{T} c_{pj} dT \qquad (7)$$

III. CFD Simulation Modeling, Setup and Boundary Conditions

The experimental setup consisted of convergent-divergent fins arranged as an inline and staggered arrangement mounted on the base plate located above the heater plate and the other side of the heater plate having the glass wool insulation to minimize heat loss. This complete setup was sealed in a wooden box, except the fins. The same setup was modeled in the CFD analysis as per the dimensions and details provided in the technical paper [1].

As per the details in [1], the model for the convergent-divergent fins (inline and staggered arrangement), the 3-d model of the geometry, hexahedral and tetrahedral mesh with mesh sizes of 0.001m to 0.15m were created and a total of 5.9 million mesh cells were obtained. The prepared 3-d model and geometrical information with mesh is shown in Figs. 1 and 2. The boundary conditions and material property details are shown in Table 1.

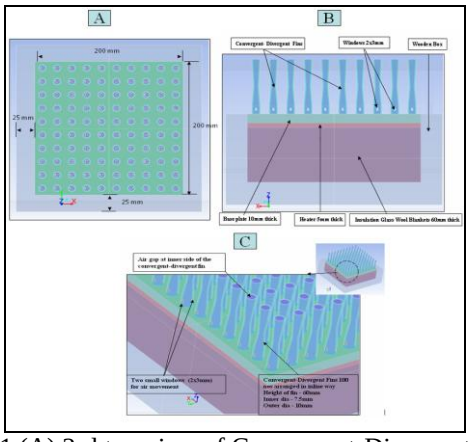

Fig. 1 (A) 2-d top view of Convergent-Divergent Fins, (B) side view of Convergent-Divergent Fins, (C) zoomed view of Convergent-Divergent Fins all (inline arrangement)

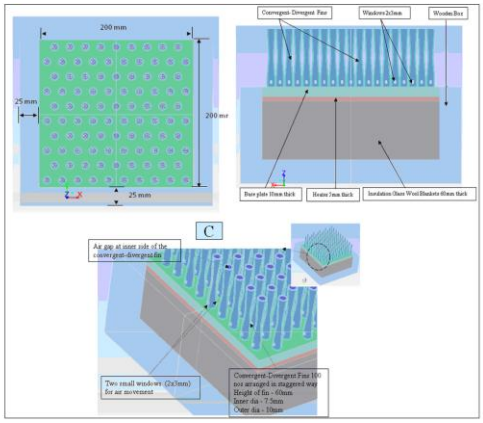

Fig. 2 (A) 2-d top view of Convergent-Divergent Fins, (B) side view of Convergent-Divergent Fins, (C) zoomed view of Convergent-Divergent Fins all (staggered arrangement)

Table 1 Boundary Conditions and Material Properties

Boundary Conditions and Material Properties					
S. No	Components	Material	Properties		
			Density Kg/m^3	Thermal Conductivity W/m-K	Specific Heat J/kg-K
1	Heater, Fins, Base Plate	Aluminium	2770	237	896
2	Insulation	Glass Wool	15	0.04	670
3	Wooden Box	King Wood	550	0.13	2000
4	Ambient Temperature 20^0C				
5	Air velocity 0.05 m/s				

As per the boundary conditions, geometry information and material properties mentioned in Table 1, the CFD analysis for the inline and staggered arrangement was carried out for 8 different power inputs of heater plate, as shown in Table 2, to see the temperature distribution on the base plate and fins surfaces due to effect of natural convection.

Table 2 Number of Heat Power Input

S. No	Heater Power (in W)	Heater Heat Flux (in W/m^2) for 200mm x 200mm heater size
1	10	250
2	20	500
3	30	750
4	50	1250
5	70	1750
6	90	2250
7	110	2750
8	130	3250

IV. Results and Discussion

4.1 CFD simulation for inline arrangement

Fig. 3 below shows the temperature contour at the base plate, wooden box and fins from the isometric view of the Convergent-Divergent Fins (inline arrangement) for different types of heat flux. Fig. 4 shows the temperature plot for the base plate and

fins as Convergent-Divergent Fins (inline arrangement).

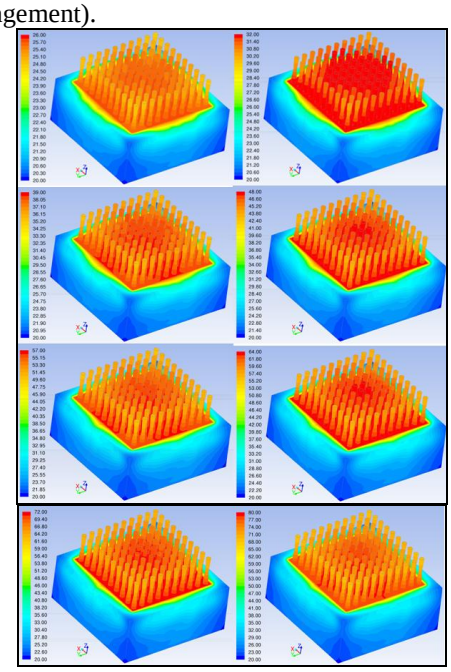

Fig. 3 Temperature contour at the base plate, wooden box and fins from the isometric view of the Convergent-Divergent Fins (inline arrangement) for different types of heat flux

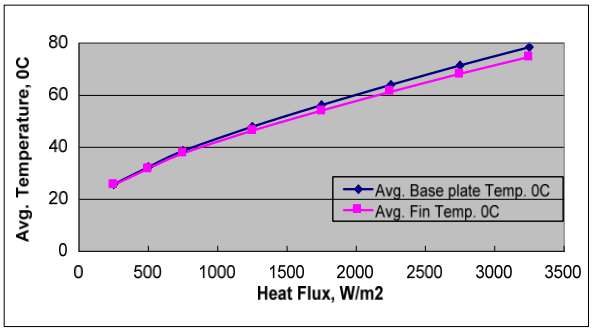

Fig. 4 Plot of temperature for base plate and fins in Convergent-Divergent Fins (inline arrangement)

As is evident from the plot shown in Fig. 4, the average fin temperature matches the average base plate temperature quite closely at lower values of heat flux, but drops below that of the base plate at higher flux values. This is the expected result because the amount of heat lost would increase with the increasing values of heat flux. Table 3 shows the comparison between numerical values of the average base plate temperature and the average fin surface temperature.

Table 3 Inline Arrangement CFD Results

Heat Power in Watts	Heat Flux in W/m^2	Average Base Plate Temperature ^{0}C (in CFD)	Average Fins Surface Temperature ^{0}C (in CFD)
10	250	25.74	25.47
20	500	32.40	31.81
30	750	38.57	37.64
50	1250	47.88	46.36
70	1750	56.21	54.12
90	2250	64.03	61.37
110	2750	71.48	68.26
130	3250	78.53	74.75

The base plate temperatures obtained in CFD analysis and experiments for inline arrangement were shown and are compared in Table 4 below.

Table 4 Comparison of CFD and Experimental Results

Heat Power in Watts	Heat Flux in W/m^2	Average Base Plate Temperature in ^{0}C (in CFD)	Average Base Plate Temperature in ^{0}C (in Experiment)	Temperature Difference in ^{0}C (CFD-Experiment)
10	250	25.74	26.5	-0.76
20	500	32.40	30.0	2.40
30	750	38.57	33.5	5.07
50	1250	47.88	40.5	7.38
70	1750	56.21	47.0	9.21
90	2250	64.03	52.5	11.53
110	2750	71.48	57.0	14.48
130	3250	78.53	61.5	17.03

4.2 CFD simulation results for staggered arrangement

Fig. 5 below shows the temperature contour at the base plate, wooden box and fins from the isometric view of the Convergent-Divergent Fins (inline arrangement) for different types of heat flux. Fig. 6 shows the temperature plot for the base plate and fins in Convergent-Divergent Fins (staggered arrangement).

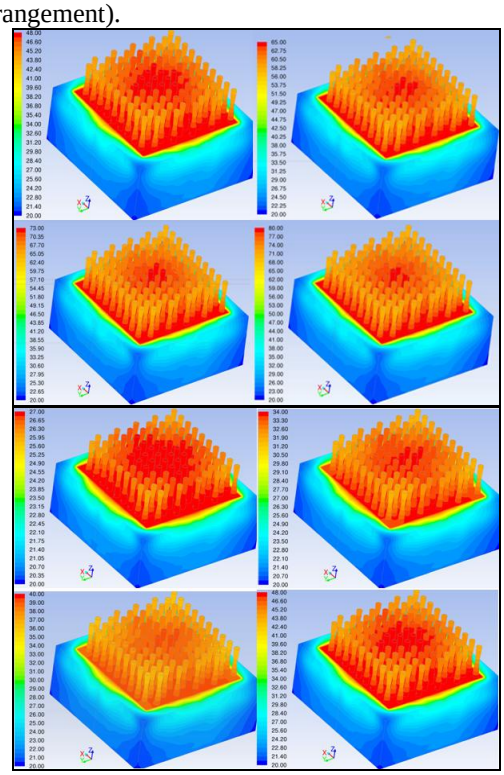

Fig. 5 Temperature contour at the base plate, wooden box and fins from the isometric view of the

Convergent-Divergent Fins (staggered arrangement) for different heat flux

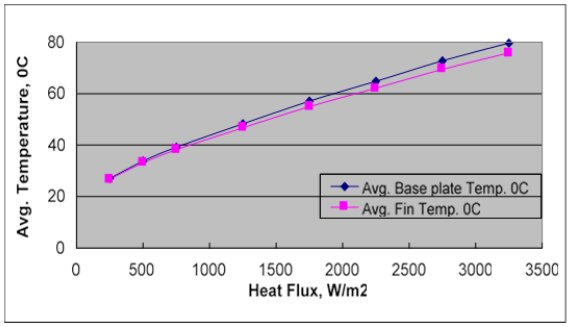

Fig. 6 Plot of Temperature for base plate and fins in Convergent-Divergent Fins (staggered arrangement)

As expected, the profile of the average fin temperature closely matches that of the average base plate temperature as in the inline arrangement case at lower heat flux values and diverges at higher flux values. Table 5 shows the CFD results for the staggered arrangement.

Table 5 Staggered Arrangement CFD Results

Heat Power in Watts	Heat Flux in W/m^2	Average Base Plate Temperature ^{O}C (in CFD)	Average Fins Surface Temperature ^{O}C (in CFD)
10	250	27.07	26.77
20	500	33.77	33.14
30	750	39.18	38.24
50	1250	48.26	46.74
70	1750	57.05	54.93
90	2250	64.81	62.14
110	2750	72.71	69.43
130	3250	79.67	75.85

The base plate temperatures obtained in the CFD analysis and experiments for the staggered arrangement were shown and are compared in Table 6.

Table 6 Base Plate CFD Results

Heat Power in Watts	Heat Flux in W/m^2	Average Base Plate Temperature in ^{O}C (in CFD)	Average Base Plate Temperature in ^{O}C (in Experiment)	Temperature Difference in ^{O}C (CFD-Experiment)
10	250	27.07	27.0	0.07
20	500	33.77	32.0	1.77
30	750	39.18	37.5	1.68
50	1250	48.26	46.0	2.26
70	1750	57.05	55.0	2.05
90	2250	64.81	62.5	2.31
110	2750	72.71	69.0	3.71
130	3250	79.67	74.5	5.17

V. Conclusions from CFD Simulation Results

The CFD steady state simulations were carried out for 'Convergent-Divergent Fins (inline and staggered arrangement)' in order to compare the base plate temperature obtained in the experimental results with the CFD results.

As per the above table, for inline, the base plate temperature results obtained in the CFD analysis for heat power ranges from 10 to 130 watts was 0.3 to 7% higher than the temperature obtained in the experimental results.

As per the above table for staggered, it is evident that the base plate temperature results obtained in the CFD analysis for heat power ranges from 10 to 130 watts and was -2 to 27% higher than the temperature obtained in experimental results.

References

[1] M. M. Awad, Assessment of Convergent-Divergent Fins Performance In Natural Convection, *Journal of American Science, 9(2)*, 2013.

[2] A. B. Dhumne and H. S. Farkade, Heat Transfer Analysis of Cylindrical Perforated Fins in Staggered Arrangement, *International Journal of Innovative Technology and Exploring Engineering, 2(5)*, 2013.

[3] L. Li, X. Du, L. Yang, Y. Zu and Y. Yang, Numerical simulation on flow and heat transfer of fin structure in air-cooled heat exchanger, *Applied Thermal Engineering, 59(1–2)*, 2013, 77–86.

[4] T. Asim, R. Mishra, K. Ubbi and K. Zala, Computational Fluid Dynamics Based Optimal Design of Vertical Axis Marine Current Turbines, *Proc. Procedia CIRP 11*, 2013, 323–327.

[5] E. Sigurdsson, K. M. Ingvorsen, M. V. Jensen, S. Mayer, S. Matlok and J.H. Walther, Numerical analysis of the scavenge flow and convective heat transfer in large two-stroke marine diesel engines, *Applied Energy, 123*, 2014, 37–46.

[6] J. H. Ferziger and M. Perić, *Computational methods for fluid dynamics* (Berlin: Springer-Verlag, 1996).

[7] H. Versteeg and W. Malalasekera, *An Introduction to Computational Fluid Dynamics: The Finite Volume Method (2nd ed.)* (Harlow: Pearson Education Ltd, 2007).

[8] J. Anderson, *Computational Fluid Dynamics* (McGraw-Hill Science, 1995).

[9] G. Cox, Compartment Fire Modelling, in G. Cox (Ed.), *Combustion Fundamentals of Fire* (Academic Press, 1995) 329-404.